Machine Learning for the Classification of Saturn Kilometric Radiation using Cassini data

E.P. O'Dwyer[1], C.M. Jackman[1], K. Domijan[2], and L. Lamy[3]

[1]Dublin Institute for Advanced Studies, Ireland [2]Maynooth University, Ireland [3]LESIA, France

1.ABSTRACT

Saturn Kilometric Radiation (SKR) is an auroral emission that occurs between a few kHz to 1.5MHz, and peaks in the frequency range 100-400 kHz. It was detected quasi-continuously by Cassini from its arrival at Saturn in 2004 until mission end in 2017 and its properties have been extensively studied. SKR bursts which are global intensifications of SKR as well as extensions of the main SKR band down to lower frequencies, known as Low Frequency Extensions (LFEs), result from internally-driven tail reconnection and from solar wind compressions of the magnetosphere, which also trigger tail reconnection. LFEs have been selected by eye and also using a numerical criterion based on an intensity threshold [Reed et al., 2018]. In our work we propose to develop a supervised machine learning algorithm to select SKR bursts with an associated LFE from the entire Cassini dataset. The algorithm would be developed using Cassini RPWS (radio instrument) data and trained with a diverse dataset that includes examples of LFEs detected from a broad range of spacecraft locations.

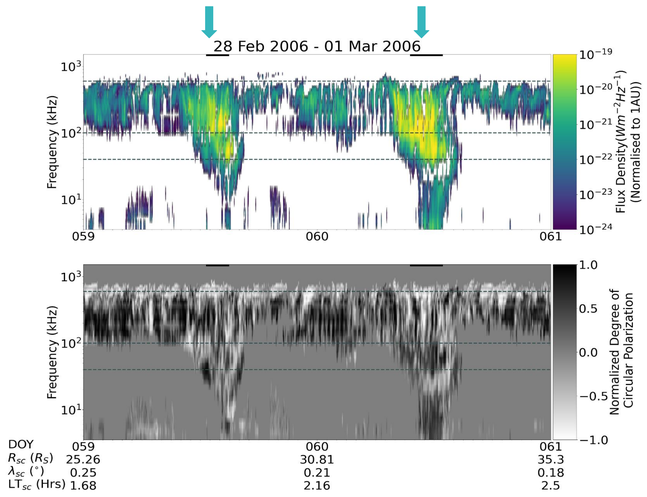

Figure 1: *Cassini RPWS spectrogram showing flux density (top) and polarization (bottom). Frequencies 40 kHz, 100 kHz and 600 kHz are indicated by dotted lines. LFE occurrence (start to stop times) according to criterion by Reed et al 2018 indicated by heavy black lines at the top of the plot.*

2. SPACECRAFT VIEWING CONDITIONS

Impact of spacecraft location on the observed radio emission.

- SKR is generated by accelerated electron beams in auroral zones by the Cyclotron Maser Instability and is beamed out in hollow cones with sources located along field lines of invariant latitude ≥ 70° [Lamy et al, 2008].
- This leads to a strong dependence of SKR visibility on spacecraft location, in particular an 'equatorial shadow zone', a region near the equator where SKR emission cannot be detected due to anisotropic beaming of SKR [Lamy et al, 2008].
- In figure (2), we present plots of the trajectory of Cassini in 2006 (top) and 2008 (bottom).
- In 2006, Cassini spent the majority of the time at equatorial latitudes, passed through all local times and reached distances of > 68R_S down Saturn's magnetotail.
- In 2008, Cassini is much closer to the planet (<40 R_S) but is mostly at higher latitudes. Orbit duration was shorter, and associated rate of passage through different viewing regions was quicker than in 2006.
- There is a high diversity in the radio signatures observed in 2006 and 2008 due to the variation in spacecraft location, making these years ideal datasets for the training data.

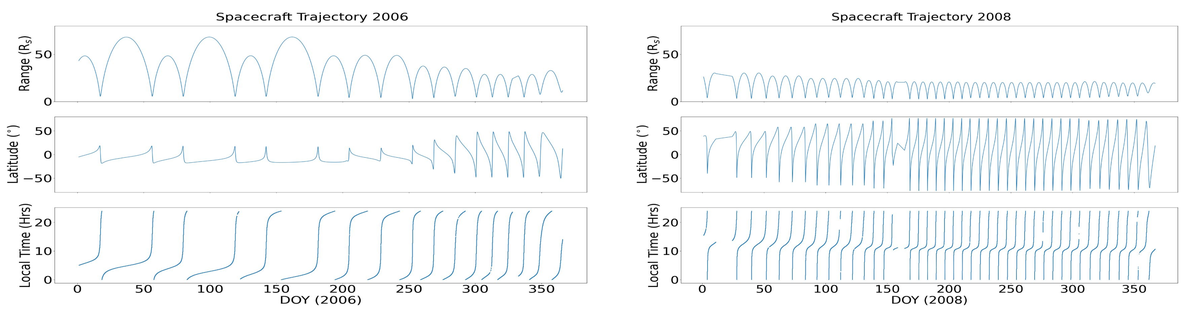

Figure 2: *Spacecraft trajectory in 2006 (left) and 2008 (right).*

3. Examples of LFE's.

- Due to the strong dependence of spacecraft location on the visibility of SKR, the radio signature of LFE's varies drastically with spacecraft location, particularly at high latitudes.
- To account for this, the colorbars of the spectrograms are normalised to within the 10th and 80th percentiles of its given Latitude and Local Time (LT) range. The data is split into two Latitude ranges: $|\lambda_{SC}| < 5°$and $|\lambda_{SC}| > 5°$, and 4 LT ranges: 0-6, 6-12, 12-18 and 18-24 Hrs LT.
- The LFE selection is done using the polygon selector tool by Empey et. al [2021]. LFE's may be one of two classes: type 1 and type 2.
- Type 1 LFE is the standard type with intense emission extending continuously from the main band down to lower frequencies. Type 2 LFE's consist of LFE's that become extinct at high latitudes due to the anisotropic beaming of SKR, and LFE's with slightly varied intensity throughout, resulting in a sparse appearance.

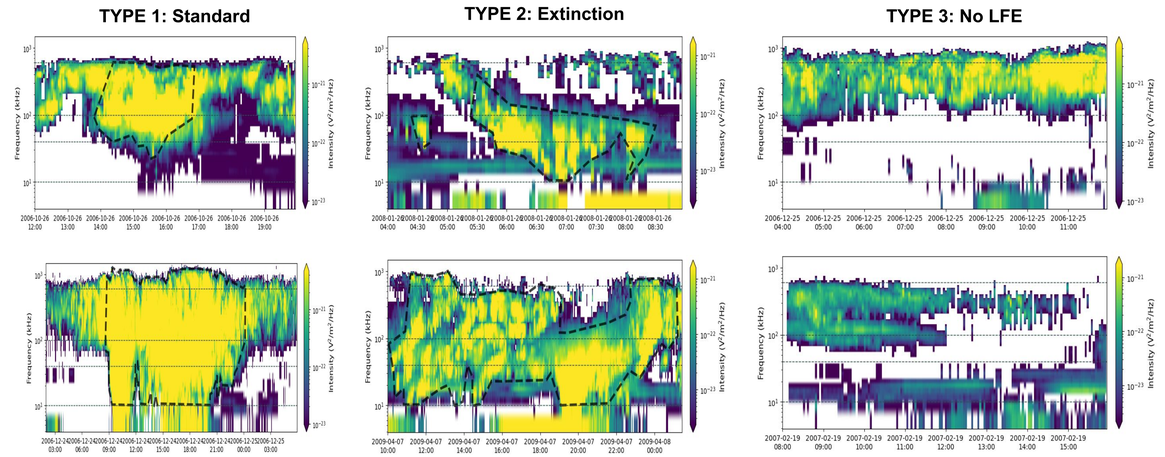

Figure 3: *Cassini RPWS Spectrograms showing flux density for the three classifications, LFE, LFE with extinction at high frequencies and No LFE.*

4. PRELIMINARY CLASSIFICATION RESULTS

- Below are the results of two neural networks used for classification of LFE images. A feedforward neural net (FFNN) and convolutional neural net (CNN) were used. The networks classified 3 different classes, as .
- The dataset used consisted of 1019 images in total, with 815 in the training set and 204 in the test set. 25% of the training data (204 images) were used as the validation set.
- The FFNN reached an accuracy of 93% on the training set and 89% on the test set.
- The CNN reached an accuracy of 96% on the training set and 87% on the test set.

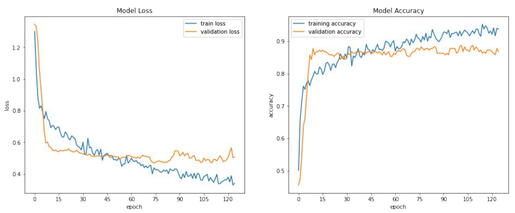

Figure 4: *The structure of the CNN used in this figure consists of a convolutional layer with 2 filters (each of dimension 1x5), a batch normalization layer, a max pooling layer (2x4 filter size) and then 2 dense layers with 'Relu' activation and 10 and 25 nodes respectively. The final layer has 3 nodes and 'softmax' activation, which allows us to interpret the predictions as the probability of each class.*

The model ran for 125 epochs, with a mini-batch size of 25. Stochastic Gradient Descent, 'SGD', was used as an optimizer.

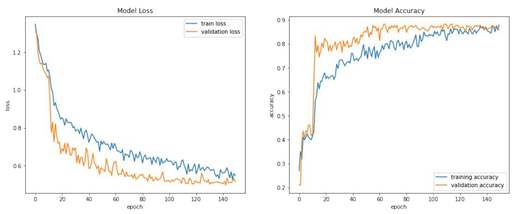

Figure 5: *The structure of the FFNN used in this figure consists of 2 dense layers with 'Relu' activation and 10 and 25 nodes respectively. The final layer has 3 nodes and 'softmax' activation, which allows us to interpret the predictions as the probability of each class.*

The model ran for 125 epochs, with a mini-batch size of 25. Stochastic Gradient Descent, 'SGD', was used as an optimizer.

5.NEXT STEPS

- Complete labelling of training data set.
- Split data into train/test validation sets
- Explore both image-based and time series methods.
- Ultimate output will be a complete set of LFEs covering the entire Cassini mission with scope to learn about the physics of the auroral acceleration region, and link between LFEs and magnetospheric dynamics

6. REFERENCES

Reed, J. J., Jackman, C. M., Lamy, L., Kurth, W. S., & Whiter, D. K. (2018). Low-frequency extensions of the Saturn Kilometric Radiation as a proxy for magnetospheric dynamics. Journal of Geophysical Research: Space Physics, 123, 443– 463. https://doi.org/10.1002/2017JA024499 ;Lamy, L., Zarka, P., Cecconi, B., Prangé, R., Kurth, W. S., and Gurnett, D. A. (2008), Saturn kilometric radiation: Average and statistical properties, J. Geophys. Res., 113, A07201 doi: https://doi.org/10.1002/2017JA024499 ; Aaron Empey, Corentin K. Louis, & Caitriona M. Jackman. (2021). SPACE Labelling Tool (1.1.0). Zenodo. https://doi.org/10.5281/zenodo.5636922